Prediction of the energy dissipation rate in ductile crack propagation

Atkins, A. G.; Chen, Zhong; Cotterell, Brian

2003

Atkins, A. G., Chen, Z., & Cotterell, B. (2003). Prediction of the Energy Dissipation Rate in Ductile Crack Propagation. Fatigue & Fracture of Engineering Materials & Structures, 26(1), 67-77.

https://hdl.handle.net/10356/94040

https://doi.org/10.1046/j.1460-2695.2003.00599.x

Prediction of the energy dissipation rate in ductile crack propagation

A. G. ATKINS[1], Z. CHEN[2] and B. COTTERELL[3]
[1]Department of Engineering, University of Reading, Reading RG6 6AY, UI,
[2]School of M aterials Engineering,
Nanyang Technological University, Singapore 639798,
[3]Department of echanical Engineering, University of Sydney, NSW 2006, Australia
Correspondence: A. G. Atkins, Department of Engineering, University of Reading,
Reading RG6 6AY, UK. E-mail: a.g.atkins@reading.ac.uk

ABSTRACT

In this paper, energy dissipation rate D vs. Δa curves in ductile fracture are predicted using a 'conversion' between loads, load-point displacements and crack lengths predicted by NLEFM and those found in real ELPL propagation. The NLEFM/ELPL link was recently discovered for the DCB testpiece, and we believe it applies to other cracked geometries. The predictions for D agree with experimental results. The model permits a crack tip toughness $R(\Delta a)$ which rises from J_c and saturates out when (if) steady state propagation is reached after a transient stage in which all tunnelling, crack tip necking and shear lip formation is established. J_R is always greater than the crack tip $R(\Delta a)$ and continues to rise even after $R(\Delta a)$ levels off.

The analysis is capable of predicting the usual D vs. (Δa) curves in the literature which have high initial values and fall monotonically to a plateau at large Δa. It also predicts that D curves for CCT testpieces should be higher than those for SENB/CT, as found in practice. The possibility that D curves at some intermediate Δa may dip to a minimum below the levelled-off value at large Δa is predicted and confirmed by experiment. Recently reported D curves that have *smaller* initial D than the D-values after extensive propagation can also be predicted. The testpiece geometry and crack tip $R(\Delta a)$ conditions required to produce these different-shaped D vs. Δa curves are established and confirmed by comparison with experiment.

The energy dissipation rate D vs. Δa is not a transferable property as it depends on geometry. The material characteristic $R(\Delta a)$ may be the 'transferable property' for scaling problems in ELPL fracture. How it can be deduced from D vs. Δa curves (and by implication, J_R vs. Δa curves) is established.

Keywords

ductile cracking at large Δa; ductile fracture; elastoplastic fracture; energy dissipation rate; J_R curves.

INTRODUCTION

It is well known that J_R resistance curves at much greater Δa than permitted by J-control

(i) depend upon starting (a_o/W) in a given testpiece and
(ii) are different for different types of testpiece.

At small Δa, where data overlap and there is experimental error, these dependencies are not always clear, although there has been growing evidence for point (ii) even at small Δa. This lack of uniqueness in J_R curves has raised doubt not only as to whether a rising J_R curve is a material property and 'transferable', but also whether a rising J_R curve really does mean increased resistance to crack propagation. Differences in J_R curves are often explained away by constraint arguments (T, Q). Alternatively, new methods of analysis have been put forward, of which the value of D is one.[a]

Accumulated irreversible work, from first loading to some known crack propagation length, is the link in ductile fracture mechanics between *D* and the *plastic* part of J_c and J_R [e.g. Turner[1], Turner and Kolednik[2]]. It is well-known that for crack initiation (Fig. la)

$$J_c^p = \eta U_{init}^p / B b_0 \qquad (1)$$

and for crack propagation (Fig. lb)

$$J_R^p = \eta\left(U_{init}^p + U_{prop}^p\right)/B b_0 = \eta\left(U_{acc}^p\right)/B b_0 \qquad (2)$$

Also,

$$D = \frac{d(U_{init}^p + U_{prop}^p)}{B d(\Delta a)} = \frac{d\left(U_{acc}^p\right)}{B d(\Delta a)} \qquad (3)$$

In the above η may vary with (a/W); also for grooved testpieces having net ligament thickness B_n, B is replaced by B_n. (This applies for all subsequent relations too).

We note that there are other, slightly different, definitions and/or ways of evaluating J_R^p such as the Ernst integral[3] and the ASTM procedure for incrementing U_{prop}^p for J_R^p.[4] These differences are not important for the thrust of the present paper. However, as pointed out by Memhard *et al.*[5] it is important to know how different parameters were determined when making comparisons between J_c^p, J_R^p and *D*.

[a] Note that we employ the symbol *D* for the energy dissipation rate; some authors[5] employ the symbol *R*. We reserve *R* for crack tip toughness, following standard practice in LEFM and NLEFM.

Typical shapes of J_R^p vs. Δa and D vs. Δa are shown in Fig. 2, taken from the experimental results in Ref. [6]. The Figure also shows numerical predictions for D vs. Δa by Siegmund and Brocks.[6]

Clearly there must be a relationship between D given by Eq. (3) and J_R^p given by Eq. (2) which is

$$U_{acc} = B \int_{a_0}^{a} D\,d(\Delta a) \qquad (4)$$

so, when η is constant (independent of (a/W) as in deeply notched bending)

$$J_R = \frac{\eta}{b_0} \int_{a_0}^{a} D\,d(\Delta a) \qquad (5)$$

or,

$$D = \frac{b_0}{\eta} \frac{dJ_R}{d(\Delta a)} \qquad (6)$$

We see from Eq. (6) that the large initial values of D at small Δa in Fig. 2 correspond with initially steep J_R curves at small Δa. At increased Δa, $dJ_R/d(\Delta a)$ diminishes and sometimes tends to a constant slope; this is where the D vs. Δa curve levels out.

The relationships between J_R^p and D predicted by Eqs (4)—(6) have been investigated and quantified by Memhard *et al.*[7] using a variety of experimental results, including cases where η varies with (a/W), as in the compact tension (CT) testpiece; in these cases, Eqs (4)—(6) were modified to include η varying and the differential equations were solved. These relationships are, of course, between curves derived from the same experimental load-displacement-propagated crack length data and, in that sense, there is an 'inevitability' about the relations. The problem remains of how to predict J_R and D curves from first principles. The present paper does this for D. A discussion of how to predict J_R curves is contained by Cotterell *et al.*[8] and will be the subject of future papers. The analysis uses a new result discovered recently in the exact algebraic closed-form solution of elastoplastic crack propagation in the double cantilever beam testpiece.[9] This result 'converts' the crack propagation part of the fully reversible path-independent algebraic NLEFM solution for the problem, to the only partially reversible path-dependent elastoplastic propagation solution. In the DCB geometry it is possible to straightforwardly separate the local crack tip work of fracture and the remote plastic work, which is not the case for other cracked bodies. We believe that the same connection may apply to other cracked geometries.[8] Note that computational methods using crack tip cohesive zone models, in particular, implicitly partition total work into these two work components.

To predict D, we need first to predict U_{acc}. We do that first for true NLEFM where displacements are globally reversible, since this forms the starting point of the later elastoplastic solution.

TRUE NLEFM

We require a relationship between load (X), fully reversible load-point displacement (u) and crack area (A). Experiments show that 'variables-separable' relationships work well, i.e. where the dependence of X~u on A is uncoupled. Various different functions have been advocated, such as simple power law relations, power-linear relations[10] relations derived from the EPRI handbook[11] and so on. (Most of these X, u, A relations have, of course, been advocated for *elastoplastic* behaviour but given the equivalence of NLEFM and Hencky total strain plasticity up to crack initiation[12] we use them here; for true NLE FM experiments and calculations, see Gurney & Ngan[13]).

For purposes of illustration we shall use

$$X = C\,(b/W)^z\,(u/W)^n \qquad (7)$$

where b is ligament length (b = (W-a)), and W is the total width of the sample; z, n and C are constants. The EPRI estimation analyses[11] may be shown to follow this type of variables-separable power law, particularly for high values of the work hardening index N in the Ramberg - Osgood version of the material work hardening relation $(\varepsilon/\varepsilon_0) = \alpha(\sigma/\sigma_0)^N$ where ε is true strain, σ is true stress and α is a constant. The index n in Eq. (7) is (1/N).

We follow the standard procedures of NLEFM[13] i.e.

$$U_{\text{init}} = \int X\,\mathrm{d}u = \frac{C}{(n+1)}(b/W)^z\left(\frac{u^{n+1}}{W^n}\right) \qquad (8)$$

and for cracking at crack tip toughness R

$$R = -\left(\frac{\partial U_{\text{init}}}{B\,\partial a}\right)_u = +\left(\frac{\partial U_{\text{init}}}{B\,\mathrm{d}b}\right)_u \qquad (9)$$

In a grooved testpiece leaving a net section thickness of B_n, B in Eq. (9) is replaced by B_n. Hence

$$R = \frac{+zC}{B(n+1)}\left(\frac{b}{W}\right)^{z-1}\left(\frac{u}{W}\right)^{n+1} \qquad (10)$$

using Eq. (8) where u in Eq. (10) is the displacement at which cracks initiate having starter length b and, equivalently, since true NLEFM is path independent, u is the current load-point displacement for a propagating crack having current length b. R need not be constant during propagation, of course: if $R(\Delta a)$ is known, Eq. (10) will give u during cracking$_G$ at $\Delta a = (b_0 - b)$.

In terms of η we have, using Eqs (8) and (10)

$$\eta = \frac{RBb_0}{U_{\text{init}}} = z \qquad (11a)$$

which is independent of (a/W) for the relation (7) Landes and coworkers[14] have pointed out this simple connexion between η and z for a power-law variables-separable X, u, A relation. Propagation need not occur at constant crack tip toughness, but Eq. (10) will always give the current value of R. Equation (11a) transposes to

$$R = \frac{\eta U_{\text{init}}}{Bb_0} \qquad (11b)$$

and this, too, will always give the correct R. Notice however, that Eq. (11b) employs U_{init} and *not* U_{acc}, the significiance of which will emerge later. That is, in Fig. 3(A),

$$R_C = \eta\overline{\text{OCD}}/Bb_1 \quad R_E = \eta\overline{\text{OEF}}/Bb_2 \quad R_G = \eta\overline{\text{OGH}}/Bb_3$$

The external work done during propagation in true NLE FM is given by

$$U_{\text{prop}}^{\text{nle}} = \int X \, \mathrm{d}u \qquad (12)$$

during propagation, so

$$\mathrm{d}u = \frac{u}{n+1}\left(\frac{\mathrm{d}R}{R} - (z-1)\frac{\mathrm{d}b}{b}\right) \qquad (13)$$

whence, in Eq. (12) and using Eqs (7) and (10)

$$U_{\text{prop}}^{\text{nle}} = \frac{B}{z}\int [b \, \mathrm{d}R - (z-1)R \, \mathrm{d}b] \qquad (14)$$

Notice that the non-linearity given by n has disappeared: Eq. (14) is in fact purely geometric. $U_{\text{prop}}^{\text{nle}}$ obviously depends on the form of crack tip $R(\Delta a)$. For the moment, let us take R as a constant = R_0 (we shall employ variable R later). Then

$$U_{\text{prop}}^{\text{nle}} = +(z-1)\frac{B}{z}R_0\int \mathrm{d}(\Delta a) \qquad (15)$$

since db = -d(Δa). The accumulated work is thus

$$\begin{aligned} U_{\text{acc}}^{\text{nle}} &= U_{\text{init}} + U_{\text{prop}}^{\text{nle}} \\ &= \frac{R_0 B b_0}{z} + (z-1)\frac{R_0 B \Delta a}{z} \end{aligned} \qquad (16a)$$

using Eqs (15) and (11).[b] But in true NLEFM, some of this accumulated work is recoverable. It is given by $R_0Bb/z = R_0B(b_0-\Delta a)/z$. Whence the dissipated work is given by

$$\begin{aligned} U_{\text{diss}} &= \frac{R_0 B b_0}{z} + (z-1)\frac{R_0 B \Delta a}{z} - \frac{R_0 B (b_0 - \Delta a)}{z} \\ &= R_0 B \Delta a \end{aligned} \qquad (16b)$$

It follows from Eq. (3) that D in true NLEFM is

$$D = R_0 \qquad (17)$$

at constant crack tip toughness and this is independent of the power law index *n*. The result is sensible, in that the only dissipated work is the crack tip toughness work.

REAL ELASTOPLASTIC PROPAGATION AND TRUE NLEFM

The equivalence of NLEFM and Hencky total strain plasticity[12] permits loads or displacements at crack *initiation* in elastoplastic cracking to be predicted, but the lacuna is how to predict the path-dependent loads and displacements during *propagation* where the NLEFM/ Hencky total strain plasticity connexion is lost as soon as the load falls.

We recently published the exact, closed-form, solution for elastoplastic crack propagation in the DCB testpiece.[9] In this special cracked geometry, the remote plastic work can be uncoupled from the local crack tip work. That cannot be done easily in other cracked geometries, which is why there are no algebraic (*X*, *u*, *A*) relations known for elastoplastic crack propagation under decreasing load in other cracked bodies. In comparing and contrasting the NLEFM solution for the DCB problem and our elastoplastic crack propagation solution, we showed that *extra work*

[b] When η is permitted to vary – no longer employing Eq. (7) for the load (*X*)-load-point displacement (*X*)-crack length (*A*) relationship – it may be shown[8] that $\mathrm{d}U_{\text{acc}}^{\text{nle}} = R + \mathrm{d}/\mathrm{d}a[bR/\eta]$.

had to be performed in the elastoplastic case compared with the true NLEFM case to achieve the same Δa because not all the energy stored in the arms of the test-piece is recovered; in true NLEFM all such work is recovered and the only dissipated work is the crack-tip fracture work. This meant that the load-point displacements during propagation under decreasing load were greater in elastoplastic cracking than in NLE FM. The connexions between work and displacements in the two cases are algebraically exact for the DCB geometry.

The link between fully reversible NLEFM and path-dependent ELPL may be expressed in the following terms. During propagation we have for NLEFM

$$(X\,\mathrm{d}u)^{\mathrm{nle}} = \mathrm{d}U^{\mathrm{nle}} + R\,\mathrm{d}A \qquad (18)$$

and for ELPL,

$$(X\,\mathrm{d}u)^{\mathrm{elpl}} = \mathrm{d}U^{\mathrm{elpl}} + R\,\mathrm{d}A \qquad (19)$$

Let us write $U = (\text{mean work/vol})(\text{vol}) = wV$, whence

$$(X\,\mathrm{d}u)^{\mathrm{nle}} = w^{\mathrm{nle}}\,\mathrm{d}V + V\,\mathrm{d}w^{\mathrm{nle}} + R\,\mathrm{d}A \qquad (20)$$

and,

$$(X\,\mathrm{d}u)^{\mathrm{elpl}} = w^{\mathrm{elpl}}\,\mathrm{d}V + V\,\mathrm{d}w^{\mathrm{elpl}} + R\,\mathrm{d}A \qquad (21)$$

For propagation over a decreasing ligament, as in three-point bending, Fig. 4, dV is negative. In NLEFM negative $w^{\mathrm{nle}}\,\mathrm{d}V$ is permissible as it represents the incremental recovery of stored elastic energy in d6. But in ELPL $w^{\mathrm{nle}}\,\mathrm{d}V$ must be set at zero as there is no *recovery* from the plastic part of the deformation zone. Putting $w^{\mathrm{nle}}\,\mathrm{d}V$ = 0 and subtracting Eq. (20) from (21) we obtain

$$(X\,\mathrm{d}u)^{\mathrm{elpl}} - (X\,\mathrm{d}u)^{\mathrm{nle}} = -w^{\mathrm{nle}}\,\mathrm{d}V + V(\mathrm{d}w^{\mathrm{elpl}} - \mathrm{d}w^{\mathrm{nle}}) \qquad (22)$$

where we recognize that the NLE and ELPL work densities are strictly different.

Furthermore, to a very good approximation $X^{\mathrm{elpl}} = X^{\mathrm{nle}} = X$ which has the value of the work hardening collapse load for the ligament [e.g. Hu & Albrecht,[15] Miller[16]8 given by Eq. (7) Hence

$$X\,\mathrm{d}u_{\mathrm{extra}} = -w^{\mathrm{nle}}\,\mathrm{d}V + V(\mathrm{d}w^{\mathrm{elpl}} - \mathrm{d}w^{\mathrm{nle}}) \qquad (23)$$

in which u_{extra} is the additional irreversible displacement beyond the NLEFM displacement, i.e. the total ELPL load-point displacement is given by ($u_{\mathrm{nle}} + u_{\mathrm{extra}}$).

The full solution of Eq. (23) is discussed elsewhere[17] but we note that if $dw^{elpl} \approx dw^{nle}$, Eq. (23) reduces to:

$$X\,du_{extra} = -w^{nle}\,dV = -(U^{nle}/V)\,dV \qquad (24)$$

in which (U^{nle}/V) is the mean NLEFM/Hencky deformation plasticity work density, Fig. 3(b).[18] Since dV is negative over reducing ligaments, $-w^{nle}$ dV is a positive quantity, and du_{xtra} is positive. Equation (24) gives a lower bound on X du_{extra} since $dw^{elpl} > dw^{nle}$.[17] We shall use the simpler Eq. (24) rather than Eq. (23) in what follows to produce ELPL solutions from the corresponding NLEFM solutions, and hence give algebraic expressions for D.

ELASTOPLASTIC TESTPIECES

Constant crack tip toughness

We assume that the initial non-linear loading lines are given by Eq. (7) where the displacements are now irreversible. Any recoverable elastic displacements have already been removed from displacements u, in accordance with Eq. (3). Equation (7) now represents the work hardening collapse load across the ligament, and z will be determined by the geometry of the body, e.g. z = 2 for bending; z = 1 for CCP testpieces.

To maintain generality, assume that $V \propto b^{q}$ (Fig. 4) in which case $dV/V = q^{db/b}.U^{nle}$ is the NLEFM U_{init} at different (a/W) and is given by Eq. (8). Equation (24) therefore yields

$$X\,du_{extra} = \frac{-C}{(n+1)}\left(\frac{b}{W}\right)^{z}\frac{u_{nle}^{n+1}}{W^{n}}\frac{q\,db}{b} = \frac{q}{z}RB\,da \qquad (25)$$

after substituting for u_{nle}^{n+1} from Eq. (10).

For $R = R_0$ = constant (at the J_c initiation value) throughout propagation

$$U_{extra} = +\frac{q}{z}R_0 B\Delta a \qquad (26)$$

The accumulated irreversible work in elastoplastic crack propagation with constant crack tip toughness during propagation is given by the sum of Eqs (16) and (26) i.e.

$$U_{acc}^{p} = \frac{R_0 B b_0}{z} + (z + q - 1)\frac{R_0 B\Delta a}{z} \qquad (27)$$

It follows that D from Eq. (3) becomes

$$D = \left(\frac{z + \mathrm{q} - 1}{z}\right) R_0 \qquad (28)$$

Changing crack-tip toughness *R*(Δ*a*)

In what follows, note carefully that $R(\Delta a)$ is a crack-tip characterizing parameter associated with tunnelling, shear lip formation, etc. Unlike J_R it does not include the remote plastic work during propagation. Hence J_R vs. Aa always lies above $R(\Delta a)$, and J_R continues to rise even after $R(\Delta a)$ saturates out when (if) shear lips are fully formed.

U_{init} is always given by Eq. (11). U_{prop}^{nle} by Eq. (14). U_{extra} is given by Eq. (25). Hence U_{acc}^{elpl}, given by the sum of these three equation becomes

$$\begin{aligned} U_{acc}^{elpl} &= \frac{R_0 B b_0}{z} + \frac{B}{z}\int [b\,\mathrm{d}R - (z + \mathrm{q} - 1)R\,\mathrm{d}b] \\ &= \frac{B}{z}\left[(bR - b_0 R_0) + (z + \mathrm{q})\int R\mathrm{d}(\Delta a)\right] \end{aligned} \qquad (29)$$

Hence,

$$\begin{aligned} D &= \frac{\mathrm{d}U_{acc}^{elpl}}{B\,\mathrm{d}a} \\ &= \frac{1}{z}\left\{b\frac{\mathrm{d}R}{\mathrm{d}a} + (z + q - 1)R\right\} \end{aligned} \qquad (30)$$

When the crack tip *R* is constant, Eq. (30) reduces to Eq. (28). Note that there is a separate *D* curve for each starting ligament $b_0 = W\,[1—(a_0/W)]$ since $b = (b_o—\Delta a)$. For d*R*/da decreasing at the propagating crack tip as Δ*a* increases, the *D* curve falls from left to right, tending towards the asymptotic value given by (*z* + q-1)R/*z* when d*R*/d*a* = 0. Note also the influence of *z* on the overall height of the *D* curve: other things being equal, the levelled-out *D* for CCT testpieces (*z* = 1) are expected to be higher than for SENB testpieces (*z* = 2).

The predictions of U_{acc}^{elpl} and *D* will depend on the form taken by the cracktip $R(\Delta a)$. This has to be determined experimentally. Our experiments show that

$$R = R_0 + R_p(1 - \exp(-k\Delta a)) \qquad (31)$$

is a good candidate expression. It is very similar to the relations employed for G_R curves in LEFM. The relationship, sketched in Fig. 5, is independent of (a_0/W), but

will vary with B.[c] The form of $R(\Delta a)$reflects changing constraint at the crack tip. Saturation of $R(\Delta a)$ occurs when, in ductile fracture, shear lips have been fully developed, tunnelling is complete and the crack is propagating in steady-state. (Whether steady-state propagation is achieved depends upon cracked geometry, for example whether the ligament is long enough). The saturation R level is given by (R_0 +R_p) in Eq. (31). R_0 is the same as J_c. The distance over which the change in $R(\Delta a)$ occurs is determined by the parameter k: large k indicates a rapid rise, vice-versa for small k; (the saturated level is, theoretically, of course an asymptote). Other expressions for $R(\Delta a)$ have been investigated.[19]

Using Eq. (31) for $R(\Delta a)$, we obtain

$$U_{\text{acc}}^{\text{elpl}} = \frac{Bb_0R_0}{z} + \left(\frac{z+\text{q}-1}{z}\right)B(R_0+R_\text{p})\Delta a + \frac{BR_\text{p}}{z}\Delta a\exp(-k\Delta a) + \frac{BR_\text{p}}{z}\left[b_0 - \frac{(z+\text{q})}{k}\right][1-\exp(-k\Delta a)] \qquad (32)$$

and,

$$D = \frac{\text{d}U_{\text{acc}}^{\text{elpl}}}{B\text{d}(\Delta a)} = \frac{(z+\text{q}-1)}{z}(R_0+R_\text{p}) + \frac{R_\text{p}}{z}\exp(-k\Delta a)[k(b_0-\Delta a)-(z+\text{q}-1)] \qquad (33)$$

At $\Delta a = 0$,

$$D_{\Delta a=0} = \frac{(z+\text{q}-1)}{z}R_0 + \frac{R_\text{p}kb_0}{z} \qquad (34)$$

At very large Δa, D becomes an asmptopic value given by

$$D_\infty = \frac{(z+\text{q}-1)}{z}(R_0+R_\text{p}) \qquad (35)$$

[c] Constraint indicated by T or Q has been invoked to explain the dependence of J_R curves on (a_0/W), so it might be thought that R(Δa) should be similarly affected. Within experimental error and for $0.2 < a/w < 0.7$, say , our experiments do not reveal such a strong dependency for the crack-tip $R(\Delta A)$, as opposed to the global J_R.

Of course, the greatest crack growth can only be $\Delta a = b_0$ and not infinity, at which point

$$D_{b_0} = \frac{(z+\mathrm{q}-1)}{z}\left(R_0 + R_\mathrm{p}[1-\exp(-kb_0)]\right) \qquad (36)$$

In the case when k is large, however, the levelled-off value of D at large Δa is practically the same as that given by Eq. (35).

Differentiation of Eq. (33) gives the slope of the D(Δa) curves as

$$\frac{\mathrm{d}D}{\mathrm{d}(\Delta a)} = -kR_\mathrm{p}\exp(-k\Delta a)\left[\frac{k}{z}(b_0-\Delta a) - 1 + \frac{(2-\mathrm{q})}{z}\right] \qquad (37)$$

The slope is zero when $\Delta a = \infty$ and also when

$$\Delta a = \left(b_0 - \frac{z}{k} + \frac{(2-\mathrm{q})}{k}\right) \qquad (38)$$

A second differentiation shows that the Δa value given by Eq. (38) corresponds with a minimum in D. The magnitude is

$$D_\mathrm{min} = \frac{(z+\mathrm{q}-1)}{z}\left(R_0 + R_\mathrm{p}\right) - \frac{R_\mathrm{p}}{z}\exp((z+\mathrm{q}-2) - kb_0) \qquad (39)$$

This is *smaller* than the final asymptotic value for D. We note, in passing, that a minimum in D implies a point of inflexion in the J_R curve. This is discussed in another paper.[20]

COMPARISON WITH EXPERIMENT

For proper assessment of the new ideas presented in this paper, it is desirable to have data from a range of (a_o/W) in the same type of specimen, together with extensive crack growth. Unfortunately, most J_R curves and many D curves are given for only limited (a_0/W) - often in the range slightly shorter and slightly longer than a_0/W= 0.5 - and, owing to the perception to remain within 'J-control', Δa is usually a small fraction of b_0. We have therefore performed a number of our own experiments employing testpieces with a wider range of (a_0/W) in which the crack is propagated to extensive Δa. From the raw load (X) displacement (u) crack length (A) plots for testpieces having different b_0, U_acc may be determined and D vs. Δa curves

constructed using Eq. (3). Analysis of D curves will give values of Rp and k for Eq. (33). The method is as follows (we assume we know $J_c = R_0$).

(i) find or estimate $D_{\Delta a} = 0$ for various b_0 from which the product ($R_p k$) is given by Eq. (34).
(ii) find or estimate D_∞ or D_{b_0} whence R_p is given by Eq. (35) or (36) and the associated k is given using step (i).
(iii) predict the D vs. Δa curves for different b_0 using these R_p and k in Eq.(33).
(iv) check that there is no systematic variation in R_p and k with (a_0/W).
(v) in the absence of systematic variations, fine-tune R_p and k to get best fits for all separate D curves using the same R_p and k.
(vi) Also, if there are minima in the D curves at smaller Δa than the levelled out values, use Eqs (38) and (39) to obtain additional estimates of R_p and k.

When J_R curves are available for the same data, it is possible to find the best pair of R_p and k-values that make the algebra for J_R (given in Ref. [20]) fit the experimental curves. (Checks should be made here too for systematic variations of R_p and k with (a_0/W)). Since J_R and D are derived from the same data for U_{acc} - Equations (2), (3), (5) and (6) - it is expected that the best values should be the same. The acid test for the analysis is however, that the *same* Rp and k obtained from best-fitting the D and J_R curves must also satisfactorily predict the X, u, A load-displacement-crack length data for all (a_0/W). We find that this seems to be the case.[20] Figure 6 shows schematically the relationship between the NLEFM initiation solution for given a_0 and the subsequent propagation paths, viz: NLEFM with constant R= J_c; NLEFM with $R(\Delta a)$ given by Eq. (31) and the ELPL solution with R (Δa) given by Eq. (31) which is obtained from the NLEFM solution using the 'additional work' line of attack.

We have performed three-point bend tests on 50%- side-grooved 12 mm thick HE30TF aluminium alloy (similar to 6165) using standard methodology, but with a wide range of (a_0/W)and extensive Δa. Figure 7(a) shows the load-plastic component of displacement-crack length results for three-point bend testpieces having (a_0/W)= 0.2, 0.4, 0.6, 0.8 where W= 50 mm and the span S = 200 mm. The associated D curves for each (a_0/W)are shown in Fig. 7(b). The J_R curves for each (a_0/W)are presented elsewhere.[20] Using z = q = 2 in Eq. (33) for D, and in other algebra for J_R and the loaddisplacement-crack length X, u, A curves[20] it is found that the following $R(\Delta a)$ well represents the (X, u, A), D and JR results for all (a_0/W)investigated, viz:

$$R = 80 + 220[1-\exp(-400\Delta a)]\text{kJ m}^{-2} \quad (\Delta a \text{ in m}) \tag{40}$$

Note in Fig. 7(a) that the crack initiation points at different (a_0/W)marked by arrows all lie on the NLEFM constant R= 80 kJ m^{-2} locus, but that subsequent propagation follows different paths.

Steady-state propagation (defined as the attainment of constant-width central flat fracture regions) occurs after $\Delta a \approx$ 5-6 mm. At this Δa, R from Eq. (31) is rather

more than 90% of the saturated value of (R_0 + R_p)= 300 kJm^{-2}. The rise in $R(\Delta a)$ in HE30TF alloy comes about not from the formation of shear lips (the testpieces are grooved) but from crack growth across the crack front as well as along it.

Results for 50% side-grooved CT specimens made from the broken halves of the bend testpieces suggest

$$R = 78 + 150\,[1 - \exp(500\Delta a)]\text{kJ m}^{-2} \quad (\Delta a \text{ in m}) \tag{41}$$

which was also roughly the $R(\Delta a)$ relationship derived from a third set of experiments on 50% side-grooved DENT testpieces also made from the broken halves of the bend specimens.

The theoretical D curve for (a_0/W)= 0.8 in Fig. 7(b) dips below the asymptotic value of (3/2)(R_0 + R_p) = 450 kJ m^{-2} in bending. According to Eq. (38) with the parameters in (40) a minimum in D should occur at $\Delta a \sim$ 5 mm when (a_0/W) = 0.8 having value 423 kJ m^{-2}. With a stretch of imagination it might be said that the experimental result agrees, but more data are desirable. For the other (a_0/W), Eq. (38) gives larger Δa values for minima than the Δa giving the levelled-out value, so no minima are seen in D curves for the other (a_0/W). Chen *et al*.[20] shows that only the J_R curve for (a_0/W) = 0.8 has an inflexion in this particular material. We observe, in passing, that there are far fewer results for D than for J_R in the literature. Inflexions in J_R can be found in the literature and this implies minima in D at the same Δa had D curves been constructed from the same data.

Furthermore while it might be argued that the dip in D down to some 420 kJ m^{-2} shown in Fig. 7(b) is within experimental error of the asymptotic level of 450 kJ m^{-2}, data recently given by Stampfl and Kolednik[21] support the analysis of this paper by displaying marked minima in some D curves before the levelled-out value at large Δa; the associated J_R curves also inflect upwards after the Δa at the minimum, Fig. 8, for different testpiece thicknesses of plain-sided steel V720. These results also display later falls in D at larger Δa which the authors attribute to crack instability and increased crack velocity. We note that the J_R curves maintain reasonably constant slopes at large Aa. According to Eq. (6) the D curves should therefore *not* drop off as they are shown to do in Fig. 8. Clearly there is some unresolved discrepancy in this part of the diagram.

Analysis of the Stampfl and Kolednik D curves using Eqs (33)—(39) suggests something like:

$$R = 65 + 468[1 - \exp(-122\Delta a)] \quad (25\text{mm thick})$$
$$R = 65 + 1585[1 - \exp(-110\Delta a)] \quad (16\text{mm thick})$$
$$R = 65 + 2402[1 - \exp(-95\Delta a)] \quad (8\text{mm thick})$$
$$R = 65 + 3802[1 - \exp(-92\Delta a)] \quad (4\text{mm thick}) \qquad (42)$$

(all kJ m^{-2}; Δa in m). These results imply that the 'saturated' crack tip toughness given by (R_0 +R_p) is ever higher the thinner the material, but that the rate of climb from J_c = 65 kJ $^{m-2}$ is lower the thinner the sheet. Both these effects seem to be explicable on the basis of lower constraint in thinner sheets.

Inspection of Eqs (33) and (39) says that marked minima will be given when (R_p/z)exp[(z + q - 2)- kb_0] is large. This means large Rp and small (kb_0). In a given material (fixed R_0, R_p and k) minima in D will appear at small b_0; this occurs for our data in Fig. 7(b). On the other hand, for fixed b_0 as in the Stampfl and Kolednik[21] experiments, where a_0/W= 0.56 for all testpieces in their Fig. 5, dips in D curves can only come about from different R_p and k. This is what we have just calculated to give relations (42).

Stampfl and Kolednik's results[21] are additionally interesting, because they show $D_{\Delta a=0} < D_\infty$ for all cases except the thickest plate (ignoring the fall in D for some thicknesses at large Δa referred to above). Inspection of Eqs (34) and (39) shows that this can happen when

$$kb_0 < (z + q - 1) \qquad (43)$$

which, for their CT testpieces with z = q = 2, means kb_0 < 3.

All the testpieces illustrated in Fig. 8 taken from Stampfl and Kodelnik[21] have b_0 = 0.022 m. Using the k-values in relations (42) for the different thickness plates, we obtain kb_0 = 2.6 (25 mm); 2.42 (16 mm); 2.09 (8 mm); and 2.02 (4mm). The only $D_{\Delta a=0} < D_\infty$ occurs for B = 25 mm, so we should expect that kb_0 to be numerically greater than three, with all the others less than three in value. While kb_0 for B = 25 mm is, in fact, just less than three, we note that the ranking of kb_0 for all thicknesses has the correct trends, the smallest kb_0 being associated with the thinnest (4mm) plate which has the lowest $D_{\Delta a=0}$. It is worth mentioning that the R_p and k given above are values that best fit all the Eqs (33)-(39) so that they may imperfectly describe separate $D_{\Delta a=0}$, D_∞, $D_{\min}$, $\Delta a_{\min}$, etc. values.

Calculations have also been performed on the D curves given by Memhard *et al.*[5] and Siegmund and Brocks[6] to establish the values of R_p and k which would fit their data. We find
2024-T351 aluminium alloy

$R = 25 + 114[1 - \exp(-815\Delta a)]$ kJm^{-2}(SENB/CT)

$R = 25 + 280[1 - \exp(-170\Delta a)]$ kJm^{-2}(CCT)[d]

StE460 steel

$R = 111 + 250[1 - \exp(-667\Delta a)]$ $kJm^{-2}(CT)$

$R = 111 + 1300[1 - \exp(-114\Delta a)]$ $kJm^{-2}(CCT)$[d]

The CCT D curves lie above the SENB/CT D curves as shown in Fig. 2 for the steel. At the same R_p and k this is to be expected from Eq. (33) owing to the different z(=1, not 2) giving $D_\infty = 2(R_0+R_p)$ for the CCT geometry in place of $D_\infty = (3/2)(R_0+R_p)$ for the SENB/CT. In addition, however, the CCT plots have larger R_p and lower k. That is, the crack-tip growth resistance (i) rises to a higher value in the CCT testpiece, and (ii) takes a longer Δa to reach the saturated-out value. This seems to reflect the lower constraint in the CCT type of testpiece.

CONCLUSIONS

Energy dissipation rate D vs. Δa curves have been predicted at small and large Δa from the load (X)-displacement (u)-crack length (A) relation for elastoplastic crack propagation at large Δa which, in turn, has been 'converted' from the path-independent and reversible Hencky/NLEFM X, u, A solution for the same problem, by means of the requirement for 'extra work' in the real path-dependent, displacement-irreversible elastoplastic case. The 'conversion' separates the crack tip fracture work from the remote plastic work elsewhere in the test-piece. It is found that the usual shape for D vs. Δa curves (large values at small Δa, decreasing to constant values at large Δa is readily explained but, in addition, unusual-shaped D vs. Δa curves are also predicted where values at small Δa can be smaller than at large Δa and also where, even in the usual-shape D vs. Δa curve, an intermediate minimum in D can be found smaller than the levelled-off value at large Δa. The circumstances under which these unusual curves can occur depends upon the type of test-piece and its starter crack length, and upon the material parameter k in $R = R_0 + R_p (1 - \exp(-k\Delta a))$ which controls the distance over which the crack tip fracture toughness R rises from the initiation value R_0 to the steady-state plateau level of $(R_0 + R_p)$ after any tunnelling and shear lip formation has been completed.

Experimental results from a variety of sources agree with the predictions in a consistent fashion for given materials. There is a separate D curve for each starting ligament. Since D vs. Δa depends on testpiece geometry, it cannot be a 'transferable' material property. The crack tip R(Δa), uncoupled from the remote plasticity always

[d] Care is required in the interpretation of CCT (also called M(T) testpieces) regarding whether Δa is for one or both crack tips, and whether U_{acc}^{elpl} is for the whole testpiece or only half of it.

included in D and J_R curves, may be a transferable material property. It will, however, be subject to through-thickness constraint, as shown by the results of Brocks and coworkers[5,6] where constraint changed because of different types of testpiece, all of the same thickness, and by the results of Stampfl and Kolednik[21] where constraint changed because of different thickness plates of the same type of testpiece. From both approaches, we may tentatively conclude that lower constraint gives greater ($R_0 + R_p$) steady-state plateau toughness, and lower k (a less rapid rise over a greater transitional Δa from the initiation R_0 level to the plateau level). Other things being equal, small k promotes D_{min} dips, and a tendency for $D_{\Delta a=0} < D_{\infty}$. Even so, we note that the analysis predicts higher D vs. Aa curves for CCT testpieces, compared with SENB/CT testpieces of the same material and thickness (as found in experiments), even for the *same* R_p and k. It follows from Eq. (6) that differences in J_R curves between CCT and SENB/CT are to be expected, without recourse of having to invoke T or Q arguments.

Acknowledgement

Dr J. D. G. Sumpter is thanked for continuing discussions on this and related topics in ductile fracture mechanics.

REFERENCES

[1] Turner, C. E. (1990). A re-assessment of ductile tearing resistance, Part I: The geometry dependence of J_R curves in fully plastic bending. Part II: Energy dissipation rate and associated *R*-curves on normalized axes. In: *Fracture Behaviour and Design of Materials and Structures, Eighth European Conference on Fracture* Vol II, EMAS, (Edited by D. Firrao), Turin, Warley, UK, pp. 933-949, 951-968.

[2] Turner, C. E. and Kolednik. 0. (1994) A micro and macro approach to the energy dissipation rate model of stable ductile crack growth. *Fatigue Fract. Engng Mater. Struct.* **17**, 1089-1107.

[3] Ernst, H., Paris, P. C. and Landes, J. D. (1981) In: *Fracture Mechanics Proceedings of the 13th National Symposium* ASTM 743 (Edited by R. Roberts). American Society for Testing and Materials. Philadelphia, PA.

[4] ASTM, E. 1152-1187. Standard test method for determining J–R curves. In: *Annual Book of ASTM Standards*, 03.01. American Society for Testing and Materials, Philadelphia, PA.

[5] Memhard, D., Brocks, W. and Fricke, S. (1993) Characterization of ductile tearing resistance by energy dissipation rate. *Fatigue Fract. Engng Mater. Struct.* **16**, 1109-1124.

[6] Siegmund, T. and Brocks, W. (2000) A numerical study on the correlation between the work of separation and the dissipation rate in ductile fracture. Engng Fract. Mech. 67, 139-154.

[7] Memhard, D., Brocks, W. and Fricke, S. (1994) Characterisation of ductile tearing resistance by energy dissipation rate. Proc. ECF-10. 1, 149-158.

[8] Cotterell, B., Chen, Z. and Atkins, A. G. (2000) On the extension of the J_R concept to significant crack growth in multiscale deformation and fracture in materials and structures In: *The James R. Rice 60th Anniversary Volume* (Edited by T.~J. Chuan and J. W. Rudnicki). Kluwer Academic Press, Dordrecht.

[9] Atkins, A. G., Chen, Z. and Cotterell, B. (1998) The essential work of fracture and JR curves for the double cantilever beam specimen of elastoplastic crack propagation. *Proc. Roy. Soc. Lond.* A454, 815-833.

[10] Orange, T. W. (1990) In: Fracture Mechanics: 21st Symposium ASTM STP 1074. American Society for Testing and Materials, Philadelphia. PA.

[11] Kumar, V., German, M. D. and Shih, C. F. (1981) *An Engineering Approach for Elastic-Plastic* Fracture Analysis. Palo Alto, EPRI.

[12] Kachanov, L. M. (1971*) Foundations of the Theory of Plasticity*. Amsterdam, North Holland.

[13] Gurney, C. and Ngan, K. M. (1971) Quasi-static crack propagation in non-linear structures. Proc. Roy. Soc. **A325**, 207-222.

[14] Sharobeam, M. H. and Landes, J. D. (1991) The load separation criterion and methodology in ductile fracture mechanics. int. J. Fract. **47,** 81-104.

[15] Hu, J. M. and Albrecht, P. (1991) Limited load solution and loading behaviour of C(T) fracture specimen. *Int. J. Fract.* 52, 19-45.

[16] Miller, A. G. (1988) Review of limit loads of structures containing defect. int. J. Press. Vessels Piping **32**, 1-50.
[17] Cotterell, B., Zhong Chen and Atkins, A. G. (2001) The essential work of fracture concept and extra work. Submitted for publication.
[18] Atkins, A. G. (1999) Scaling laws for elastoplastic fracture. int. J. Fract. **95**, 51-65.
[19] Zhong Chen (1997) PhD Dissertation, University of Reading, Reading, UK.
[20] Zhong Chen, Cotterell, B. and Atkins, A. G. (2000) Stability of elastoplastic crack propagation at large Aa: Part 1 on JR curves. *Engng Fract. Mech*. (being revised).
[21] Stampfl, J. and Kolednik, 0. (2000) The separation of the fracture energy in metallic materials int. J. Fract. **101**, 321-345.

List of Figures

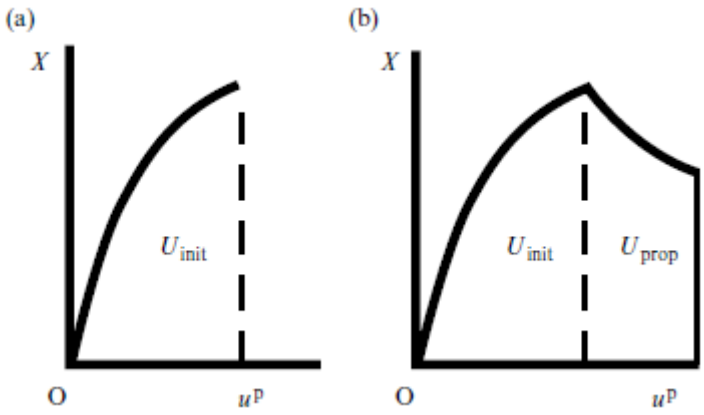

Figure 1

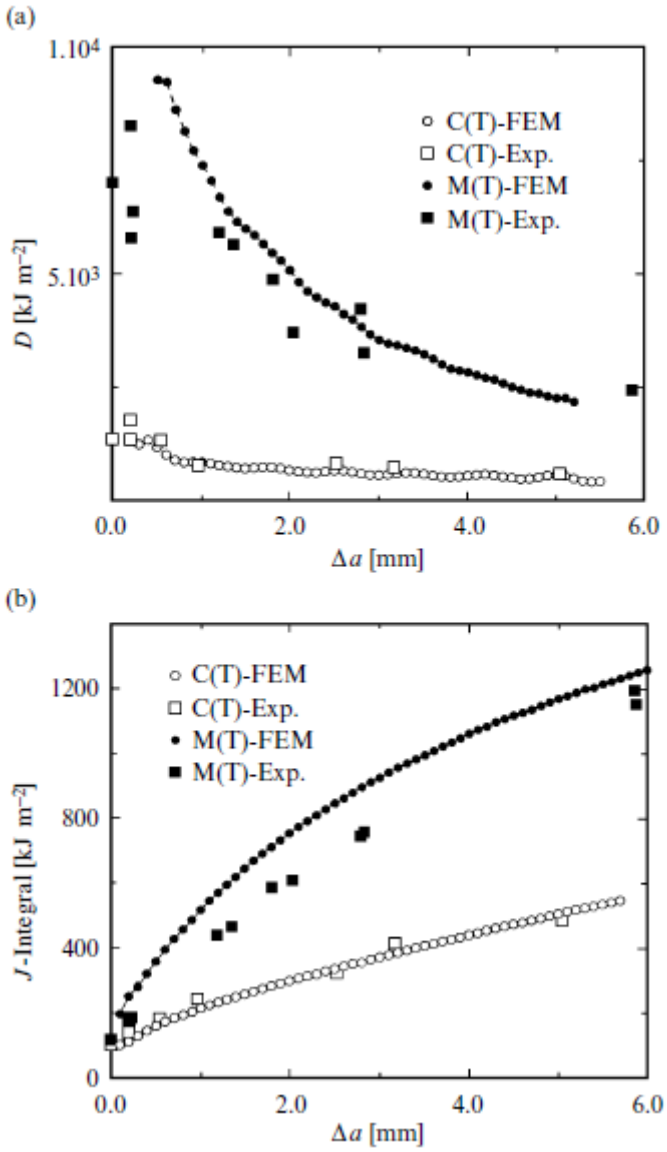
(a)
1.10⁴
5.10³
D [kJ m⁻²]
C(T)-FEM
C(T)-Exp.
M(T)-FEM
M(T)-Exp.
0.0
2.0
4.0
6.0
Δa [mm]
(b)
1200
800
400
0
J-Integral [kJ m⁻²]
C(T)-FEM
C(T)-Exp.
M(T)-FEM
M(T)-Exp.
0.0
2.0
4.0
6.0
Δa [mm]

Figure 2

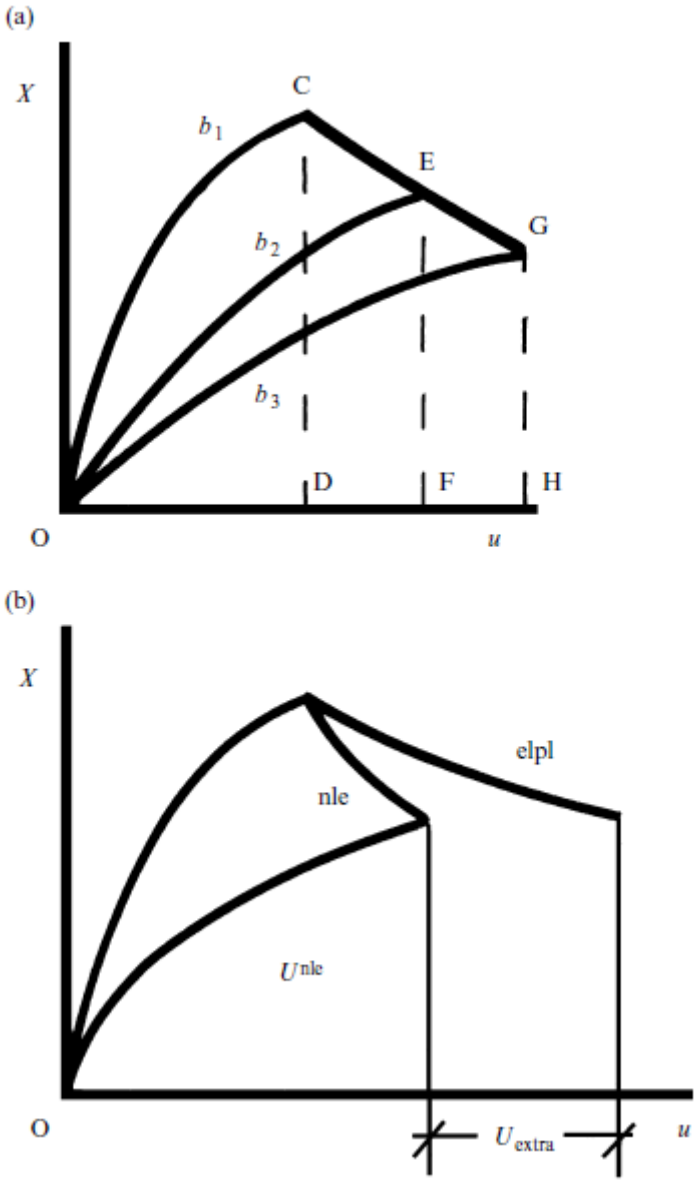

Figure 3

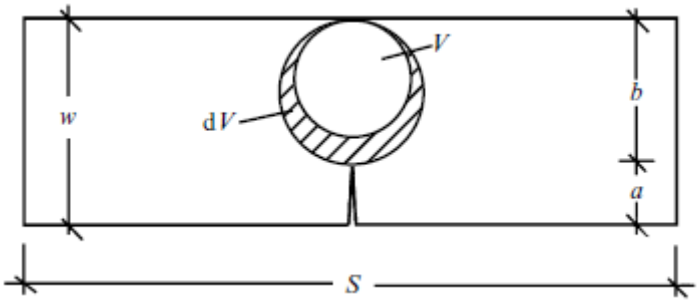

Figure 4

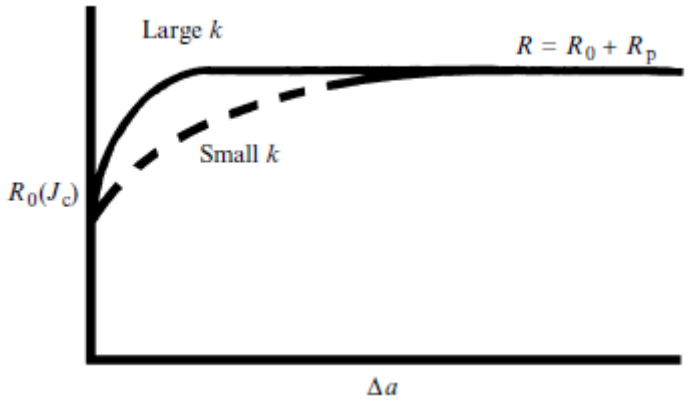

Figure 5

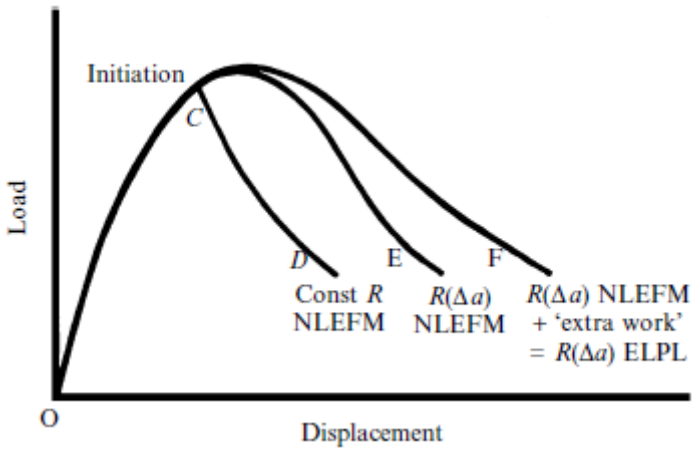
Initiation
C
D
E
F
Const R
NLEFM
R(Δa)
NLEFM
R(Δa) NLEFM
+ 'extra work'
= R(Δa) ELPL
Load
O
Displacement

Figure 6

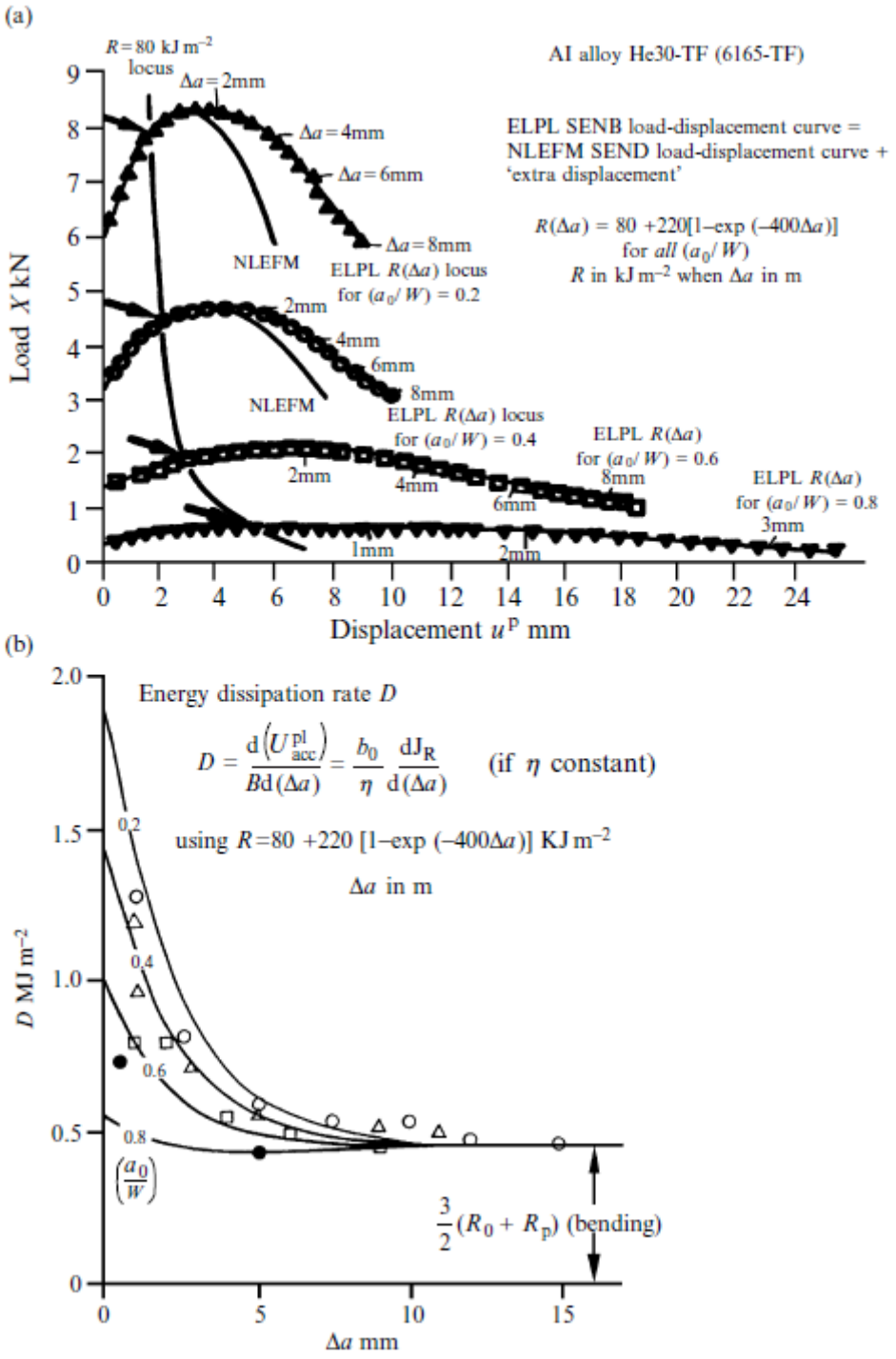
(a)
R = 80 kJ m⁻² locus
Δa = 2mm
Δa = 4mm
Δa = 6mm
Δa = 8mm
NLEFM
ELPL R(Δa) locus for (a0/W) = 0.2
2mm
4mm
6mm
8mm
NLEFM
ELPL R(Δa) locus for (a0/W) = 0.4
ELPL R(Δa) for (a0/W) = 0.6
ELPL R(Δa) for (a0/W) = 0.8
3mm
1mm
2mm
Load X kN
Displacement u^p mm
Al alloy He30-TF (6165-TF)
ELPL SENB load-displacement curve = NLEFM SEND load-displacement curve + 'extra displacement'
R(Δa) = 80 +220[1–exp (–400Δa)] for all (a0/W)
R in kJ m⁻² when Δa in m
(b)
Energy dissipation rate D
D = d(U^pl_acc) / B d(Δa) = b0/η dJR/d(Δa) (if η constant)
using R=80 +220 [1–exp (–400Δa)] KJ m⁻²
Δa in m
0.2
0.4
0.6
0.8
(a0/W)
3/2 (R0 + Rp) (bending)
D MJ m⁻²
Δa mm

Figure 7

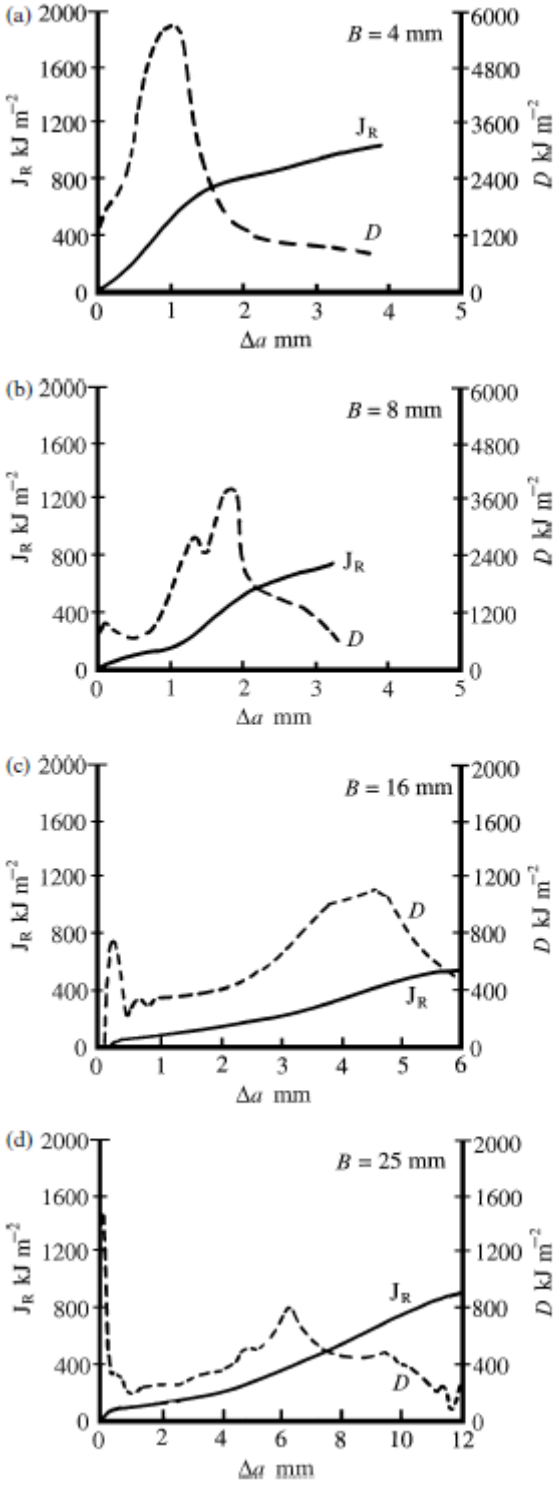
(a)
B = 4 mm
J_R
D
J_R kJ m^-2
D kJ m^-2
Δa mm
(b)
B = 8 mm
J_R
D
J_R kJ m^-2
D kJ m^-2
Δa mm
(c)
B = 16 mm
D
J_R
J_R kJ m^-2
D kJ m^-2
Δa mm
(d)
B = 25 mm
J_R
D
J_R kJ m^-2
D kJ m^-2
Δa mm

Figure 8